Transverse spin-orbit force in the spin Hall effect in ballistic semiconductor wires

Branislav K. Nikolić, Liviu P. Zârbo, and Sven Welack*
Department of Physics and Astronomy, University of Delaware, Newark, Delaware 19716-2570, USA
(Received 13 April 2005; published 12 August 2005)

We introduce the spin- and momentum-dependent force operator, which is defined by the Hamiltonian of a clean semiconductor quantum wire with homogeneous Rashba spin-orbit (SO) coupling attached to two ideal (i.e., free of spin and charge interactions) leads. Its expectation value in the spin-polarized electronic wave packet injected through the leads explains why the center of the packet gets deflected in the transverse direction. Moreover, the corresponding spin density will be dragged along the transverse direction to generate an out-of-plane spin accumulation of opposite signs on the lateral edges of the wire, as expected in the phenomenology of the spin Hall effect, when spin-↑ and spin-↓ polarized packets (mimicking the injection of conventional unpolarized charge current) propagate simultaneously through the wire. We also demonstrate that spin coherence of the injected spin-polarized wave packet will gradually diminish (thereby diminishing the "force") along the SO coupled wire due to the entanglement of spin and orbital degrees of freedom of a single electron, even in the absence of any impurity scattering.

DOI: 10.1103/PhysRevB.72.075335 PACS number(s): 72.25.Dc, 71.70.Ej, 03.65.Sq

The classical Hall effect[1] is one of the most widely known phenomena of condensed matter physics because it represents manifestation of the fundamental concepts of classical electrodynamics—such as the Lorentz force—in a complicated solid-state environment. A perpendicular magnetic field $\mathbf{B}$ exerts the Lorentz force $\mathbf{F}=q\mathbf{v}\times\mathbf{B}$ on current $\mathbf{I}$ flowing longitudinally through metallic or semiconductor wire, thereby separating charges in the transverse direction. The charges then accumulate on the lateral edges of the wire to produce a transverse "Hall voltage" in the direction $q\mathbf{I}\times\mathbf{B}$. Thus, Hall-effect measurements reveal the nature of the current carriers.

Recent optical detection[2,3] of the accumulation of spin-↑ and spin-↓ electrons on the opposite lateral edges of current carrying semiconductor wires opens new realm of the spin Hall effect. This phenomenon occurs in the absence of any external magnetic fields. Instead, it requires the presence of spin-orbit (SO) couplings, which are tiny relativistic corrections that can, nevertheless, be much stronger in semiconductors than in vacuum.[4] Besides deepening our fundamental understanding of the role of SO couplings in solids,[4,5] the spin Hall effect offers new opportunities in the design of all-electrical semiconductor spintronic devices that do not require ferromagnetic elements or cumbersome-to-control external magnetic fields.[5]

While experimental detection of the strong signatures of the spin Hall effect brings to an end decades of theoretical speculation for its existence, it is still unclear what spin-dependent forces are responsible for the observed spin separation in different semiconductor systems. One potential mechanism—asymmetric scattering of spin-↑ and spin-↓ electrons off impurities with SO interaction—was invoked in the 1970's to predict the emergence of pure (i.e., not accompanied by charge transport) spin current, in the transverse direction to the flow of longitudinal unpolarized charge current, which would deposit spins of opposite signs on the two lateral edges of the sample.[6] However, it has been argued[7] that in systems with weak SO coupling and, therefore, no spin splitting of the energy bands such spin Hall effect of the extrinsic type (which vanishes in the absence of impurities) is too small to be observed in present experiments[2] (unless it is enhanced by particular mechanisms involving intrinsic SO coupling of the bulk crystal[8]).

Much of the recent revival of interest in the spin Hall effect has been ignited by the predictions[9,10] for substantially larger transverse pure spin Hall current as a response to the longitudinal electric field in semiconductors with strong SO coupling that spin splits energy bands and induces Berry phase correction to the group velocity of Bloch wave packets.[11] However, unusual properties of such intrinsic spin Hall current in infinite homogeneous systems, which depends on the whole Fermi sea (i.e., it is determined solely by the equilibrium Fermi-Dirac distribution function and spin-split Bloch band structure) and it is not conserved in the bulk due to the presence of SO coupling,[9,10] have led to arguments that its nonzero value does not correspond to any real transport of spins[12,13] so that no spin accumulation near the boundaries and interfaces could be induced by any intrinsic mechanism (i.e., in the absence of impurities[13]).

On the other hand, quantum transport analysis of spin-charge spatial propagation through clean semiconductor wires, which is formulated in terms of genuine nonequilibrium and Fermi surface quantities (i.e., conserved spin currents[14–16] and spin densities[17]), predicts that spin Hall accumulation[2,3] of opposite signs on its lateral edges will emerge due to strong SO coupling within the wire region.[17] Such mesoscopic spin Hall effect is determined by the processes on the mesoscale set by the spin precession length,[15,17] and depends on the whole measuring geometry (i.e., boundaries, interfaces, and the attached electrodes) due to the effects of confinement on the dynamics of transported spin in the presence of SO couplings in finite-size semiconductor structures.[18,19]

Thus, to resolve the discrepancy between different theoretical answers to such a fundamental question as—*Are intrinsic SO interaction terms in the effective Hamiltonian of a clean spin-split semiconductor wire capable of generating the spin-Hall-like accumulation on its edges?*—it is highly

desirable to develop a picture of the transverse motion of spin density that would be as transparent as the familiar picture of the transverse drift of charges due to the Lorentz force in the classical Hall effect. Here we offer such a picture by analyzing the spin-dependent "force," which can be associated with any SO coupled quantum Hamiltonian, and its effect on the semiclassical dynamics of spin density of individual electrons that are injected as spin-polarized wave packets into the Rashba SO coupled clean semiconductor quantum wire attached to two ideal (i.e., interaction- and disorder-free) leads.

The effective mass Hamiltonian of the ballistic Rashba quantum wire is given by

$$\hat{H} = \frac{\hat{\mathbf{p}}^2}{2m^*} + \frac{\alpha}{\hbar}(\hat{\boldsymbol{\sigma}} \times \hat{\mathbf{p}}) \cdot \mathbf{z} + V_{\text{conf}}(y), \tag{1}$$

where $\hat{\mathbf{p}}$ is the momentum operator in two–dimensional (2D) space, $\hat{\boldsymbol{\sigma}} = (\hat{\sigma}^x, \hat{\sigma}^y, \hat{\sigma}^z)$ is the vector of the Pauli spin operators, and $V_{\text{conf}}(y)$ is the transverse potential confining electrons to a wire of finite width. We assume that the wire of dimensions $L_x \times L_y$ is realized using the 2D electron gas (2DEG), with $\mathbf{z}$ being the unit vector orthogonal to its plane. Within the 2DEG, carriers are subjected to the Rashba SO coupling of strength α, which arises due to the structure inversion asymmetry[4] (of the confining potential and differing band discontinuities at the heterostructure quantum well interface[20]).

This Hamiltonian generates a spin-dependent force operator which can be extracted[21,22] within the Heisenberg picture[23] as

$$\hat{\mathbf{F}}_H = m^* \frac{d^2 \hat{\mathbf{r}}_H}{dt^2} = \frac{m^*}{\hbar^2}[\hat{H}, [\hat{\mathbf{r}}_H, \hat{H}]]$$

$$= \frac{2\alpha^2 m^*}{\hbar^3}(\hat{\mathbf{p}}_H \times \mathbf{z}) \otimes \hat{\sigma}_H^z - \frac{dV_{\text{conf}}(\hat{y}_H)}{d\hat{y}_H}\mathbf{y}. \tag{2}$$

Here the Heisenberg picture operators carry the time dependence of quantum evolution, i.e., $\hat{\mathbf{p}}_H(t) = e^{i\hat{H}t/\hbar}\hat{\mathbf{p}}e^{-i\hat{H}t/\hbar}$, $\hat{\sigma}_H^z(t) = e^{i\hat{H}t/\hbar}\hat{\sigma}^z e^{-i\hat{H}t/\hbar}$, and $\hat{y}_H(t) = e^{i\hat{H}t/\hbar}\hat{y}e^{-i\hat{H}t/\hbar}$, where $\hat{\sigma}^z$, $\hat{\mathbf{p}}$, and $\hat{y}$ are in the Schrödinger picture and, therefore, time independent.

Since the force operator[22] depends on spin through $\hat{\sigma}_H^z$, which is an internal quantum degree of freedom,[23] it does not have any classical analog. Its physical meaning (i.e., measurable predictions) is contained in the quantum-mechanical expectation values, such as $\langle \hat{F}_y \rangle(t) = \langle \Psi(t=0) | \hat{F}_H^y(t) | \Psi(t=0) \rangle$ obtained by acting with the transverse component $\hat{F}_H^y$ of the vector of the force operator $(\hat{F}_H^x, \hat{F}_H^y)$ on the quantum state $|\Psi(t=0)\rangle$ of an electron. While such force can always be associated with a given quantum Hamiltonian, its usefulness in understanding the evolution of quantum systems is limited—the local nature of the force equation cannot be reconciled with inherent nonlocality of quantum mechanics. For example, if the force "pushes" the volume of a wave function locally, one has to find a new global wave function in accord with the boundary conditions at infinity (the same problem remains well hidden in the Heisenberg picture, where time dependence is carried by the operators while wave functions are time independent). Nevertheless, analyzing the dynamics of spin and probability densities in terms of the action of local forces can be insightful for particles described by wave packets (whose probability distribution is small compared to the typical length scale over which the force varies).[11,23]

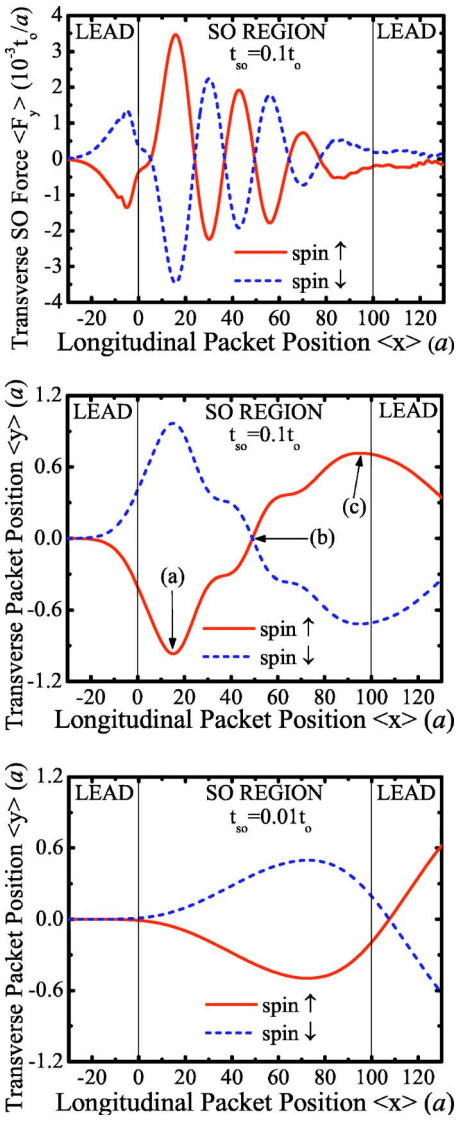

FIG. 1. (Color online) The expectation value of the transverse component of the SO force operator (upper panel) in the quantum state of propagating spin-wave packet along the two-probe nanowire. The middle panel shows the corresponding transverse position of the center of the wave packet as a function of its longitudinal coordinate. The initial state in the left lead is fully spin-polarized wave packet Eq. (3), which is injected into the SO region of the size $L_x \times L_y \equiv 100a \times 31a$ ($a \simeq 3$ nm) with strong Rashba coupling $t_{\text{SO}} = \alpha/2a = 0.1t_{\text{o}}$ and the corresponding spin precession length $L_{\text{SO}} = \pi t_{\text{o}} a/2t_{\text{SO}} \approx 15.7a < L_x$ (middle panel) or weak SO coupling $t_{\text{SO}} = 0.01t_{\text{o}}$ and $L_{\text{SO}} \approx 157a > L_x$ (lower panel).

Therefore, we examine in Fig. 1 the transverse SO force $\langle \hat{F}_y \rangle$ in the spin wave packet state, which at $t=0$ resides in the left lead as a fully spin-polarized (along the z axis) and spatially localized wave function[24,25]

$$\Psi(t=0) = C \sin\left(\frac{\pi y}{(L_y+1)a}\right) e^{ik_x x - \delta k_x^2 x^2/4} \otimes \chi_\sigma. \qquad (3)$$

This is a pure and separable quantum state $|\Psi(t=0)\rangle = |\Phi\rangle \otimes |\sigma\rangle$ in the tensor product of the orbital and spin Hilbert spaces $\mathcal{H}_o \otimes \mathcal{H}_s$. The orbital factor state $\langle x,y|\Phi\rangle$ consists of the lowest subband of the hard wall transverse confining potential and a Gaussian wave packet along the x axis whose parameters are chosen to be $k_x a = 0.44$ and $\delta k_x a = 0.1$ (C is the normalization constant determined from $\langle\Phi|\Phi\rangle = 1$). The spin factor state is an eigenstate of $\hat{\sigma}^z$, i.e., $\chi_\uparrow = \binom{1}{0}$ or $\chi_\downarrow = \binom{0}{1}$.

Unlike the case[21] of an infinite 2DEG, the exact solutions of the Heisenberg equation of motion for $\hat{\sigma}_H^z(t)$, $\hat{y}_H(t)$ and $\hat{\mathbf{p}}_H(t)$ entering in Eq. (2) are not available for quantum wires of finite width. Thus, we compute the expectation value $\langle\Psi(t)|\hat{F}_y|\Psi(t)\rangle$ in the Schrödinger picture by applying the evolution operators $e^{-i\hat{H}t/\hbar}$ present in Eq. (2) on the wave functions $|\Psi(t)\rangle = \Sigma_n e^{-iE_n t/\hbar}|E_n\rangle\langle E_n|\Psi(t=0)\rangle$. To obtain the exact eigenstates[24,26,27] $|E_n\rangle$ and eigenvalues E_n, we employ the discretized version of the Hamiltonian Eq. (1). That is, we represent the Hamiltonian of the Rashba spin-split quantum wire in the basis of states $|\mathbf{m}\rangle \otimes |\sigma\rangle$, where $|\mathbf{m}\rangle$ are s orbitals $\langle\mathbf{r}|\mathbf{m}\rangle = \psi(\mathbf{r}-\mathbf{m})$ located at sites $\mathbf{m} = (m_x, m_y)$ of the $L_x \times L_y$ lattice with the lattice spacing a (typically[19] $a \simeq 3$ nm). This representation extracts the two energy scales from the Rashba Hamiltonian Eq. (1): $t_o = \hbar^2/(2m^* a^2)$ characterizing hopping between the nearest-neighbor sites without spin flip; and $t_{SO} = \alpha/2a$ for the same hopping process when it involves spin flip.[17,19] The wave vector of the Gaussian packet $k_x a = 0.44$ is chosen[17] to correspond to the Fermi energy $E_F = -3.8t_o$ close to the bottom of the band where tight-binding dispersion relation reduces to the parabolic one of the Hamiltonian Eq. (1). In this representation one can directly compute the commutators in the definition of the force operator Eq. (2), thereby bypassing subtleties that arise when evaluating the transverse component of the force operator $-dV_{conf}(\hat{y}_H)\mathbf{y}/d\hat{y}_H$ stemming from the hard wall boundary conditions.[28]

Figure 1 shows that as soon as the front of the spin-polarized wave packet enters the strongly SO coupled region, its center $\langle\hat{y}\rangle(t) = \langle\Psi(t)|\hat{y}|\Psi(t)\rangle$ will be deflected along the y axis in the same direction as is the direction of the transverse SO force. However, due to its inertia the packet does not follow fast oscillations of the SO force occurring on the scale of the spin precession length[17,19] $L_{SO} = \pi t_o a/2t_{SO}$ on which spin precesses by an angle π (note that the spin splitting generates a finite difference of the Fermi momenta, which is the same for all subbands of the quantum wire in the case of parabolic energy-momentum dispersion, so that L_{SO} is equal for all channels[26]). In contrast to an infinite 2DEG of the intrinsic spin Hall effect,[10,12,13] in quantum wires electron motion is confined in the transverse direction and the effective momentum-dependent Rashba magnetic field $\mathbf{B}_R(\mathbf{k})$ is, therefore, nearly parallel to this direction.[19,26] Thus, the change of the direction of the transverse SO force is due to the fact that the z-axis polarized spin will start precessing within the SO region since it is not an eigenstate of the Zeeman term $\hat{\boldsymbol{\sigma}}\cdot\mathbf{B}_R(\mathbf{k})$ [i.e., of the Rashba term in Eq. (1)].

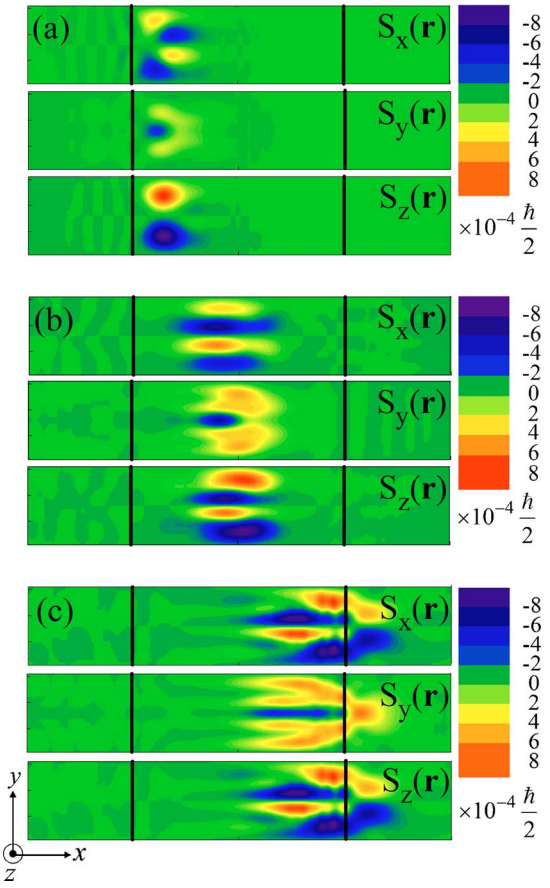

FIG. 2. (Color online) The dynamics of spin density $\mathbf{S}(\mathbf{r}) \equiv [S_x(\mathbf{r}), S_y(\mathbf{r}), S_z(\mathbf{r})]$ induced by simultaneous propagation of two electrons through quantum wire $100a \times 31a$ with the Rashba SO coupling $t_{SO} = 0.1t_o$. Both electrons are injected at $t=0$ from the left lead, one as spin-$\uparrow$ and the other one as spin-$\downarrow$ polarized (along the z axis) wave packet Eq. (3). The different snapshots of the sum of their spin densities are taken at the points (a), (b), (c), where the transverse SO force and the y coordinate of the center of these wave packets have values shown in the middle panel of Fig. 1.

The transverse SO force and the motion of the center of the wave packets in Fig. 1 suggests that when two electrons with opposite spin polarizations are injected simultaneously into the SO coupled quantum wire with perfectly homogeneous[25] Rashba coupling, the initially unpolarized mixed spin state will evolve during propagation through the wire to develop a nonzero spin density at its lateral edges. This intuitive picture is confirmed by plotting in Fig. 2 the spin density,

$$\mathbf{S}_\mathbf{m}(t) = \frac{\hbar}{2}\langle\Psi(t)|\hat{\boldsymbol{\sigma}} \otimes |\mathbf{m}\rangle\langle\mathbf{m}|\Psi(t)\rangle$$

$$= \frac{\hbar}{2}\sum_{\sigma,\sigma'} c^*_{\mathbf{m},\sigma'}(t) c_{\mathbf{m},\sigma}(t)\langle\sigma'|\hat{\boldsymbol{\sigma}}|\sigma\rangle, \qquad (4)$$

corresponding to the coherent evolution of two spin-wave

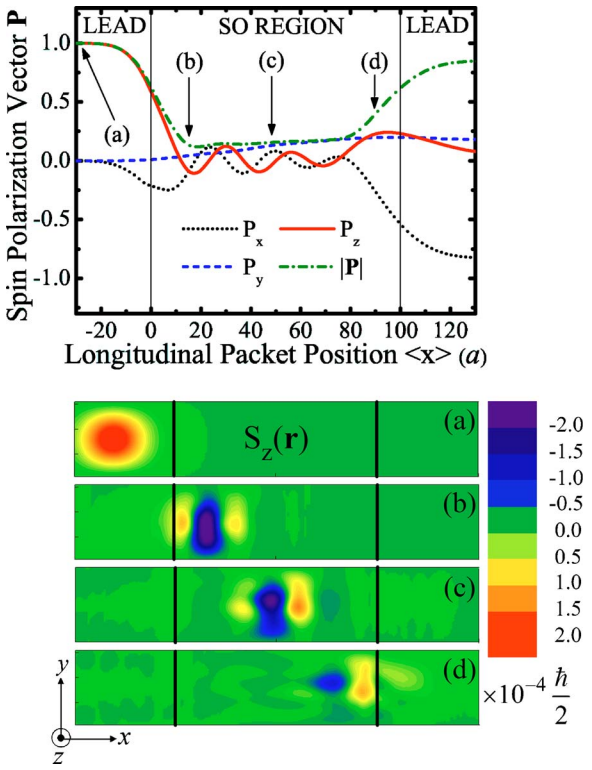

FIG. 3. (Color online) Spin precession, as signified by oscillations of the spin polarization vector (P_x, P_y, P_z), and spin decoherence (as measured by decrease of the purity $|\mathbf{P}|$ below one) of the spin state of a single electron propagating along the Rashba quantum wire $100a \times 31a$ with the SO coupling strength $t_{\mathrm{SO}} = 0.1t_{\mathrm{o}}$ ($L_{\mathrm{SO}} \approx 15.7a$). The electron is injected from the left lead as a spin-$\uparrow$ polarized wave packet, whose spin subsystem is therefore fully coherent $|\mathbf{P}|=1$ at $t=0$. The bottom panel shows the z component of the spin density $S_z(\mathbf{r})$ at different values of $(\hbar/2)P_z = \int d\mathbf{r} S_z(\mathbf{r})$ (selected in the upper panel) along the wire.

packets, $|\Psi(t=0)\rangle = |\Phi\rangle \otimes |\uparrow\rangle$ and $|\Psi(t=0)\rangle = |\Phi\rangle \otimes |\downarrow\rangle$, across the wire.

The mechanism underlying the decay of the transverse SO force intensity is explained in Fig. 3, where we demonstrate that (initially coherent) spin precession is also accompanied by spin decoherence.[19,30] These two processes are encoded in the rotation of the spin polarization vector $\mathbf{P}$ and the reduction of its magnitude ($|\mathbf{P}|=1$ for fully coherent pure states $\hat{\rho}_s^2 = \hat{\rho}_s$), respectively. The spin polarization vector is extracted from the density matrix $\hat{\rho}_s = (1 + \mathbf{P} \cdot \hat{\boldsymbol{\sigma}})/2$ of the spin subsystem.[23] The spin-density matrix $\hat{\rho}_s$ is obtained as the exact reduced density matrix at each instant of time by tracing the pure state density matrix $\hat{\rho}(t) = |\Psi(t)\rangle\langle\Psi(t)|$ over the orbital degrees of freedom,

$$\hat{\rho}_s(t) = \mathrm{Tr}_o |\Psi(t)\rangle\langle\Psi(t)| = \sum_{\mathbf{m}} \langle \mathbf{m}|\Psi(t)\rangle\langle\Psi(t)|\mathbf{m}\rangle = \sum_{\mathbf{m},\sigma,\sigma'} c_{\mathbf{m},\sigma}(t)|\sigma\rangle\langle\sigma'|c^{*}_{\mathbf{m},\sigma'}(t). \tag{5}$$

The dynamics of the spin polarization vector and the spin density shown in Fig. 3 are in one-to-one correspondence,

$$\frac{\hbar}{2}\mathbf{P}(t) = \frac{\hbar}{2}\mathrm{Tr}_s[\hat{\rho}_s(t)\hat{\boldsymbol{\sigma}}] = \sum_{\mathbf{m}} \mathbf{S}_{\mathbf{m}}(t). \tag{6}$$

The incoming quantum state from the left lead in Fig. 3 is separable, $|\Psi(t=0)\rangle = \Sigma_{\mathbf{m},\sigma} c_{\mathbf{m},\sigma}(t=0)|\mathbf{m}\rangle \otimes |\sigma\rangle = |\Phi\rangle \otimes |\uparrow\rangle$, and therefore fully spin coherent, $|\mathbf{P}|=1$. However, in the course of propagation through SO coupled quantum wires it will coherently evolve into a nonseparable[23] state where spin and orbital subsystems of the same electron appear to be entangled.[19,31] Note that Fig. 3 also shows that at the instant when the center of the wave packet enters the wire region, its quantum state is already highly entangled as quantified by the nonzero von Neumann entropy (associated with the reduced density matrix of either the spin $\hat{\rho}_s$ or the orbital subsystem $\hat{\rho}_o$),

$$S(\hat{\rho}_s) = S(\hat{\rho}_o) = -\frac{1+|\mathbf{P}|}{2}\log_2\left(\frac{1+|\mathbf{P}|}{2}\right) - \frac{1-|\mathbf{P}|}{2}\log_2\left(\frac{1-|\mathbf{P}|}{2}\right), \tag{7}$$

which is a unique measure[30] of the degree of entanglement for pure bipartite states (such as the full state $|\Psi(t)\rangle$, which remains pure due to the absence of inelastic processes along the quantum wire).

While this loss of spin coherence (or polarization) is analogous to the well-known DP spin relaxation in diffusive SO coupled systems,[5,29] here the decay of the spin polarization vector takes place without any scattering off impurities (or averaging over an ensemble of electrons propagating through ballistic SO coupled quantum dot structures[18]). Instead, it arises due to wave packet spreading (cf. lower panel of Fig. 3), as well as due to the presence of interfaces[19] (the wave packet is partially reflected at the lead-SO region interface for strong Rashba coupling) and boundaries[18,19] of the confined structure. Thus, the decoherence mechanism revealed by Fig. 3 is also highly relevant for the interpretation of experiments on the transport of spin coherence in high-mobility semiconductor[32] and molecular spintronic devices.[33]

The interplay of the oscillating and decaying (induced by spin precession and spin decoherence, respectively) transverse SO force and wave packet inertia leads to spin-$\uparrow$ electron exiting the wire with its center deflected toward the left lateral edge and the spin-$\downarrow$ density appearing on the right edge[17] for strong SO coupling $t_{\mathrm{SO}}=0.1t_{\mathrm{o}}$ in Figs. 1 and 2. This picture is only apparently counterintuitive to the naïve conclusion drawn from the form of the force operator itself Eq. (2), which would suggest that spin-$\uparrow$ electron is always deflected to the right while moving along the Rashba SO region. While such a situation appears in wires shorter than L_{SO} (as shown in the lower panel of Fig. 1), in general, one has to take into account the ratio L_x/L_{SO}, as well as the strength of the SO force $\propto \alpha^2$, to decipher the sign of the spin accumulation on the lateral edges and the sign of the corresponding spin currents that will be pushed into the transverse leads attached at those edges.[15]

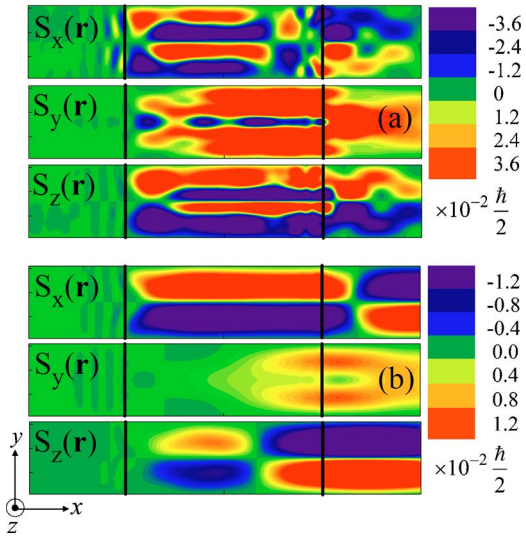

FIG. 4. (Color online) The spin accumulation $[S_x(\mathbf{r}),S_y(\mathbf{r}),S_z(\mathbf{r})]$ induced by the ballistic flow of unpolarized charge current, simulated by injecting one after another 600 pairs of spin-↑ and spin-↓ polarized (along the z axis) wave packets from the left lead, through quantum wire $100a\times 31a$ with the Rashba SO couplings: (a) $t_{\mathrm{SO}}=0.1t_{\mathrm{o}}$ ($L_{\mathrm{SO}}\approx 15.7a$) and (b) $t_{\mathrm{SO}}=0.01t_{\mathrm{o}}$ ($L_{\mathrm{SO}}\approx 157a$).

When we inject pairs of spin-↑ and spin-↓ polarized wave packets one after another, thereby simulating the flow of unpolarized ballistic current through the lead–wire–lead structure (where electron does not feel any electric field within the clean quantum wire region),[17] we find in Fig. 4 that the deflection of the spin densities of individual electrons in the transverse direction will generate nonzero spin accumulation components $S_z(\mathbf{r})$ and $S_x(\mathbf{r})$ of the opposite sign on the lateral edges of the wire. While recent experiments find $S_z(\mathbf{r})$ with such properties to be the strong signature of the spin Hall effect,[2,3] here we confirm the conjecture of Ref. 17 that $S_x(\mathbf{r})$ can also emerge as a distinctive feature of the mesoscopic spin Hall effect in confined Rashba spin-split structures—it arises due to the precession (Fig. 3) of transversally deflected spins. Note that $S_x(\mathbf{r})\neq 0$ accumulations cannot be explained by arguments based on the texturelike structure[26] of the spin density of the eigenstates in infinite Rashba quantum wires where[26,27] $S_x(\mathbf{r})\equiv 0$.

In conclusion, the spin-dependent force operator, defined by the SO coupling terms of the Hamiltonian of a ballistic spin-split semiconductor quantum wire, will act on the injected spin-polarized wave packets to deflect spin-↑ and spin-↓ electrons in the opposite transverse directions. This effect, combined with precession and decoherence of the deflected spin, will lead to nonzero z and x components of the spin density with opposite signs on the lateral edges of the wire, which represents an example of the spin Hall effect phenomenology[6,17] that has been observed in recent experiments.[2,3] The intuitively appealing picture of the transverse SO quantum-mechanical force operator (as a counterpart of the classical Lorentz force), which depends on spin through $\hat{\sigma}^z$, the strength of the Rashba SO coupling through α^2, and the momentum operator through the cross product $\hat{\mathbf{p}}\times\mathbf{z}$, allows one to differentiate symmetry properties of the two spin Hall accumulation components upon changing the Rashba electric field (i.e., the sign of α) or the direction of the packet propagation: $S_z(\mathbf{r})_{-\alpha}=S_z(\mathbf{r})_{\alpha}$ and $S_z(\mathbf{r})_{-\mathbf{p}}=-S_z(\mathbf{r})_{\mathbf{p}}$ vs $S_x(\mathbf{r})_{-\alpha}=-S_x(\mathbf{r})_{\alpha}$ (due to opposite spin precession for $-\alpha$) and $S_x(\mathbf{r})_{-\mathbf{p}}=S_x(\mathbf{r})_{\mathbf{p}}$. These features are in full accord with experimentally observed behavior of the $S_z(\mathbf{r})$ spin Hall accumulation under the inversion of the bias voltage,[3] as well as with the formal quantitative quantum transport analysis[17] of the nonequilibrium spin accumulation induced by the flow of unpolarized charge current through ballistic SO coupled two-probe nanostructures.

Finally, we note that α^2 dependence of the transverse SO force is incompatible with the α-independent (i.e., "universal") intrinsic spin Hall conductivity $\sigma_{sH}=e/8\pi$ (describing the pure transverse spin Hall current $j_y^z=\sigma_{sH}E_x$ of the z-axis polarized spin in response to the longitudinally applied electric field E_x) of an infinite homogeneous Rashba spin-split 2DEG in the clean limit, which has been obtained within various bulk transport approaches.[10–13,34] On the other hand, it supports the picture of the SO-coupling-dependent spin Hall accumulations[17] $S_z(\mathbf{r})$, $S_x(\mathbf{r})$ and the corresponding spin Hall conductances[15] (describing the z and the x component of the nonequilibrium spin Hall current in the transverse leads attached at the lateral edges of the Rashba wire) of the mesoscopic spin Hall effect in confined structures.[14–16] By the same token, the sign of the spin accumulation on the edges (i.e., whether the spin current flows to the right or to the left in the transverse direction[15]) cannot be determined from the properties[34] of σ_{sH}. Instead one has to take into account the strength of the SO coupling α and the size of the device in the units of the characteristic mesoscale L_{SO}, as demonstrated by Figs. 1 and 4. This requirement stems from the oscillatory character of the transverse SO force brought about by the spin precession of the deflected spins in the effective magnetic field of the Rashba SO coupled wires of finite width.

We are grateful to S. Souma, S. Murakami, Q. Niu, and J. Sinova for insightful discussions and E. I. Rashba for enlightening criticism. Acknowledgment is made to the donors of the American Chemical Society Petroleum Research Fund for partial support of this research.

*Present address: Institut für Physik, Technische Universität, D-09107 Chemnitz, Germany.

[1] *The Hall Effect and its Applications*, edited by C. L. Chien and C. W. Westgate (Plenum, New York, 1980).

[2] Y. K. Kato, R. C. Myers, A. C. Gossard, and D. D. Awschalom, Science **306**, 1910 (2004).

[3] J. Wunderlich, B. Kaestner, J. Sinova, and T. Jungwirth, Phys. Rev. Lett. **94**, 047204 (2005).

[4] E. I. Rashba, Physica E (Amsterdam) **20**, 189 (2004).

[5] I. Žutić, J. Fabian, and S. Das Sarma, Rev. Mod. Phys. **76**, 323 (2004).

[6] M. I. D'yakonov and V. I. Perel', Zh. Eksp. Teor. Fiz. Pis'ma Red. **13**, 657 (1971) [JETP Lett. **13**, 467 (1971)]; J. E. Hirsch, Phys. Rev. Lett. **83**, 1834 (1999); S. Zhang, *ibid.* **85**, 393 (2000).

[7] B. A. Bernevig and S.-C. Zhang, cond-mat/0412550 (unpublished).

[8] H.-A. Engel, B. I. Halperin, and E. I. Rashba, cond-mat/0505535 (unpublished).

[9] S. Murakami, N. Nagaosa, and S.-C. Zhang, Science **301**, 1348 (2003); Phys. Rev. B **69**, 235206 (2004).

[10] J. Sinova, D. Culcer, Q. Niu, N. A. Sinitsyn, T. Jungwirth, and A. H. MacDonald, Phys. Rev. Lett. **92**, 126603 (2004).

[11] D. Culcer, J. Sinova, N. A. Sinitsyn, T. Jungwirth, A. H. MacDonald, and Q. Niu, Phys. Rev. Lett. **93**, 046602 (2004); G. Sundaram and Q. Niu, Phys. Rev. B **59**, 14915 (1999).

[12] E. I. Rashba, Phys. Rev. B **70**, 161201(R) (2004); **68**, 241315(R) (2003).

[13] S. Zhang and Z. Yang, Phys. Rev. Lett. **94**, 066602 (2005).

[14] S. Souma and B. K. Nikolić, Phys. Rev. Lett. **94**, 106602 (2005).

[15] B. K. Nikolić, L. P. Zârbo, and S. Souma, cond-mat/0408693, Phys. Rev. B (to be published).

[16] L. Sheng, D. N. Sheng, and C. S. Ting, Phys. Rev. Lett. **94**, 016602 (2005); E. M. Hankiewicz, L. W. Molenkamp, T. Jungwirth, and J. Sinova, Phys. Rev. B **70**, 241301(R) (2004).

[17] B. K. Nikolić, S. Souma, L. P. Zârbo, and J. Sinova, Phys. Rev. Lett. **95**, 046601 (2005).

[18] C.-H. Chang, A. G. Mal'shukov, and K. A. Chao, Phys. Rev. B **70**, 245309 (2004); O. Zaitsev, D. Frustaglia, and K. Richter, Phys. Rev. Lett. **94**, 026809 (2005).

[19] B. K. Nikolić and S. Souma, Phys. Rev. B **71**, 195328 (2005).

[20] P. Pfeffer, Phys. Rev. B **59**, 15902 (1999).

[21] J. Schliemann, D. Loss, and R. M. Westervelt, Phys. Rev. Lett. **94**, 206801 (2005).

[22] J. Li, L. Hu, and S.-Q. Shen, Phys. Rev. B **71**, 241305(R) (2005).

[23] L. E. Ballentine, *Quantum Mechanics: A Modern Development* (World Scientific, Singapore, 1998).

[24] M. Valín-Rodríguez, A. Puente, and L. Serra, Eur. Phys. J. B **34**, 359 (2003).

[25] J. I. Ohe, M. Yamamoto, T. Ohtsuki, and J. Nitta, Phys. Rev. B **72**, 041308(R) (2005).

[26] M. Governale and U. Zülicke, Solid State Commun. **131**, 581 (2004).

[27] G. Usaj and C. A. Balseiro, cond-mat/0405065 (unpublished).

[28] D. S. Rokhsar, Am. J. Phys. **64**, 1416 (1996).

[29] M. I. D'yakonov and V. I. Perel', Fiz. Tverd. Tela (Leningrad) **13**, 3581 (1971) [Sov. Phys. Solid State **13**, 3023 (1972)]; Zh. Eksp. Teor. Fiz. **13**, 1954 (1971) [Sov. Phys. JETP **33**, 1053 (1971)].

[30] A. Galindo and A. Martin-Delgado, Rev. Mod. Phys. **74**, 347 (2002).

[31] A. Peres and D. R. Terno, Rev. Mod. Phys. **76**, 93 (2004).

[32] J. M. Kikkawa and D. D. Awschalom, Nature (London) **397**, 139 (1999).

[33] B. W. Alphenaar, K. Tsukagoshi, and M. Wagner, J. Appl. Phys. **89**, 6863 (2001).

[34] P. Zhang, J. Shi, D. Xiao, and Q. Niu, cond-mat/0503505 (unpublished).